

## Inhibited cell spreading on polystyrene nanopillars fabricated by nanoimprinting and *in situ* elongation

This article has been downloaded from IOPscience. Please scroll down to see the full text article.

2010 Nanotechnology 21 385301

(<http://iopscience.iop.org/0957-4484/21/38/385301>)

View [the table of contents for this issue](#), or go to the [journal homepage](#) for more

Download details:

IP Address: 129.110.5.91

The article was downloaded on 26/03/2011 at 23:23

Please note that [terms and conditions apply](#).

# Inhibited cell spreading on polystyrene nanopillars fabricated by nanoimprinting and *in situ* elongation

Walter Hu<sup>1,3</sup>, Adam S Crouch<sup>1</sup>, Danielle Miller<sup>2</sup>, Mukti Aryal<sup>1</sup> and Kevin J Luebke<sup>2,3</sup>

<sup>1</sup> Department of Electrical Engineering, University of Texas at Dallas, Richardson, TX 75080, USA

<sup>2</sup> Department of Internal Medicine, Division of Translational Research, University of Texas Southwestern Medical Center, Dallas, TX 75390-9185, USA

E-mail: [walter.hu@utdallas.edu](mailto:walter.hu@utdallas.edu) and [Kevin.Luebke@UTSouthwestern.edu](mailto:Kevin.Luebke@UTSouthwestern.edu)

Received 8 June 2010, in final form 14 July 2010

Published 26 August 2010

Online at [stacks.iop.org/Nano/21/385301](http://stacks.iop.org/Nano/21/385301)

## Abstract

Polymer nanopillars (40–80 nm in diameter and 100 nm in pitch) were fabricated at high density over large areas directly on bulk tissue culture polystyrene plates using nanoimprint lithography. Nanoporous Si molds for imprinting were generated by transfer from an anodic alumina membrane. Ultrahigh aspect ratio polymer nanopillars were formed in a novel procedure using controlled elongation of the imprinted pillars during mold release. The resulting nanopillar arrays show significant changes in surface wettability upon brief O<sub>2</sub> plasma treatment. Human dermal fibroblasts were cultured on the nanopillar surfaces in order to study cell–substrate interaction at the nanoscale. The nanopillar topography shows strong effects on the cell morphology, with pillars of widely varying aspect ratios and surface energies resisting cell spreading. This effect on cell behavior can be rationalized in terms of the cells' requirement to form micron-scale focal adhesions. The study indicates that at the nanoscale, physical factors can supersede the effects of chemical factors on the cell–substratum interaction.

(Some figures in this article are in colour only in the electronic version)

## 1. Introduction

Nanostructures and nanostructured biomaterials are increasingly important for applications in tissue engineering, bio-devices and systems, nanomedicine, and fundamental studies of cell biology [1–5]. The abundance of nanoscale features in the extracellular matrix has generated significant interest in the role of nanostructures in guiding cell behavior. Previous studies have characterized the behaviors of a variety of cell-types on nanoscale gratings. Many of these studies have investigated the sensitivity of cells to nanoscale features, fabricated using chemical methods and lithography [6–12]. Cell behavior on microscale pillars and nanoscale pits has also been studied, with the finding that cell adhesion varies with topographic and chemical changes [13, 14]. Despite significant achievements in this area, a comprehensive understanding

of the cell–substratum interaction at the nanoscale remains unrealized. The challenges in this area are due to the intrinsic complexity of biological systems, and importantly, to the lack of cost-effective methods to build complex nanoscaffolds of precisely controlled dimensions and surface energies. Nonetheless, an in-depth understanding of cell–substratum interactions at the nanoscale is crucial to tissue engineering as well as to the design of materials for medical devices that contact live cells.

In this paper, we demonstrate a nanoimprint method using a nanoporous Si mold to create high density ( $10^{10}$  cm<sup>-2</sup>) nanopillars or vertical nanowires of various aspect ratios (up to 25) over large areas (6 cm<sup>2</sup>) directly on tissue culture polystyrene (TCPS). Using a novel elongation process during release of the mold from the substrate, nanopillars as tall as 1 μm (twice the mold depth) can be made. Rational variation of the demolding temperature controls the length of the pillars, enabling creation of a topography that is practically

<sup>3</sup> Authors to whom any correspondence should be addressed.

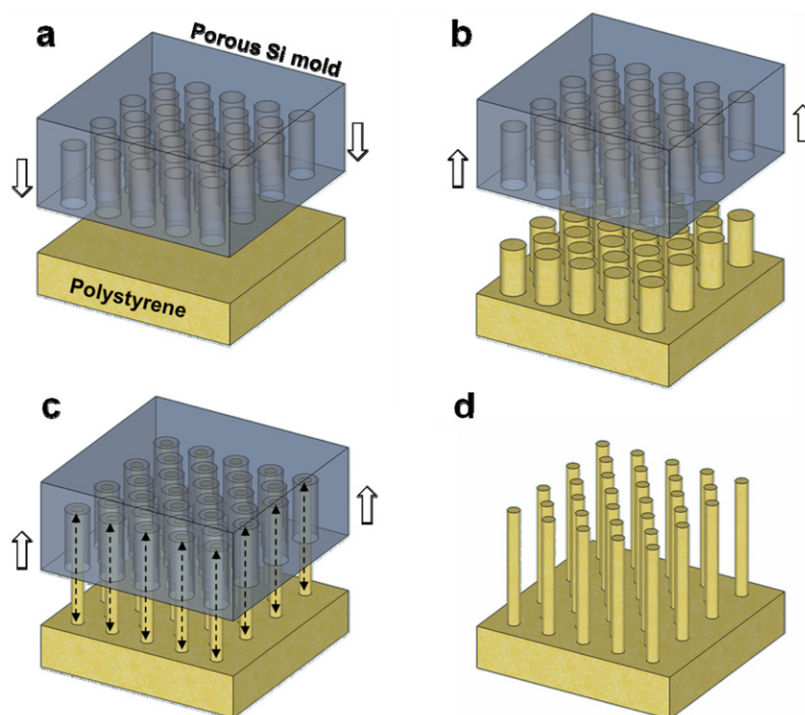


**Figure 1.** Schematic of nanoimprint schemes to create nanopillars: (a) nanoimprint with porous Si mold on a polystyrene plate; (b) conventional demolding; (c) elongation demolding with *in situ* pillar stretching; (d) elongated nanopillars with ultrahigh aspect ratio.

impossible to obtain using conventional lithographic methods. The aspect ratio of the nanopillars directly affects the surface energy of the imprinted material, tall pillars being highly hydrophobic. In contrast, a brief  $O_2$  plasma treatment renders them superhydrophilic (zero water contact angle). The resulting nanotopography combines ordered nanostructures with widely differing surface energies, providing a unique platform to study cell–substrate interactions. Human dermal fibroblasts were cultured on these substrates. Patterning of the surface with nanoscale pillars had a pronounced effect on cell morphology, independent of surface energy. Cell spreading was significantly diminished on both hydrophobic and hydrophilic surfaces that bear nanopillars. This result suggests that surfaces that resist cell spreading can be made by creating the appropriate nanoscale topography, without concern for the effect of surface chemistry on hydrophilicity.

## 2. Methods

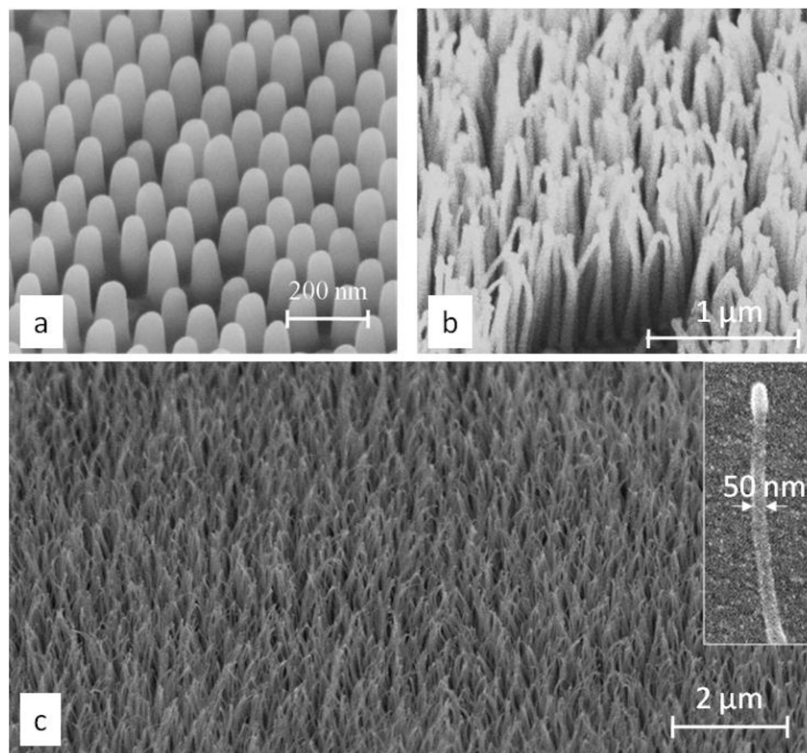
### 2.1. Nanoimprint with *in situ* elongation

Figure 1 shows two imprint methods: direct nanoimprinting on TCPS with conventional demolding (figure 1(b)) and nanoimprinting followed by demold-induced feature elongation (figure 1(c)). By varying the imprint conditions, the percentage of the mold filled by the polymer can be well-controlled. Lower temperature and/or shorter imprinting time can be used to obtain partial filling of the mold, resulting in pillar height shorter than the mold depth. Pillars of height larger than the mold depth are obtained by elongation of the pillars during mold release (figure 1(c)). Using a temperature of  $150^\circ\text{C}$ , the mold is completely filled with polystyrene

in 10–15 min. Adhesion forces of the pillar tops with the Si result in an axial tension during vertical withdrawal of the mold from the polystyrene. At temperatures where the nanopillars are still soft, this tension elongates the pillars. The extent of pillar elongation can be controlled by varying the demolding temperature. During pillar elongation, pillar diameter decreases simultaneously with increasing height, conserving pillar volume, as shown from SEM imaging. Fabrication of nanoporous Si molds is critical to this method of achieving high density and ordered nanopillars over large areas, and e-beam lithography is impractically expensive and slow for creation of these molds. Instead, free-standing anodized aluminum oxide (AAO) membranes were placed on top of the Si substrate as etch masks, and plasma etching was used to create 100 nm spaced pores in Si of 80 nm in diameter and 500 nm in depth. Detailed processing control and image results are presented in our previous work [15].

### 2.2. Cell seeding, imaging, data analysis

Human foreskin fibroblasts (HFF CRL 2522, ATCC) were maintained in Dulbecco's modified Eagle Medium (DMEM; Gibco) with 10% heat-inactivated Fetal Bovine Serum (FBS; Sigma). Prior to reaching confluence, the fibroblasts were harvested from monolayer culture with 0.25% trypsin/EDTA (Sigma). Trypsin was neutralized with 10% FBS in DMEM. Each substrate was sterilized with 70% ethanol. Fibroblasts (<15 doublings) were seeded onto the substrates at a density of  $5000\text{ cells ml}^{-1}$  in DMEM supplemented with 10% FBS. After 24 h, the cells were fixed using 4% paraformaldehyde. The cells were then processed for fluorescent staining of actin filaments and nuclei with TRITC-conjugated Phalloidin



**Figure 2.** 45° tilted SEM views of nanopillars in TCPS with heights of (a) 150 nm, (b) ~700 nm, and (c) 1 μm.

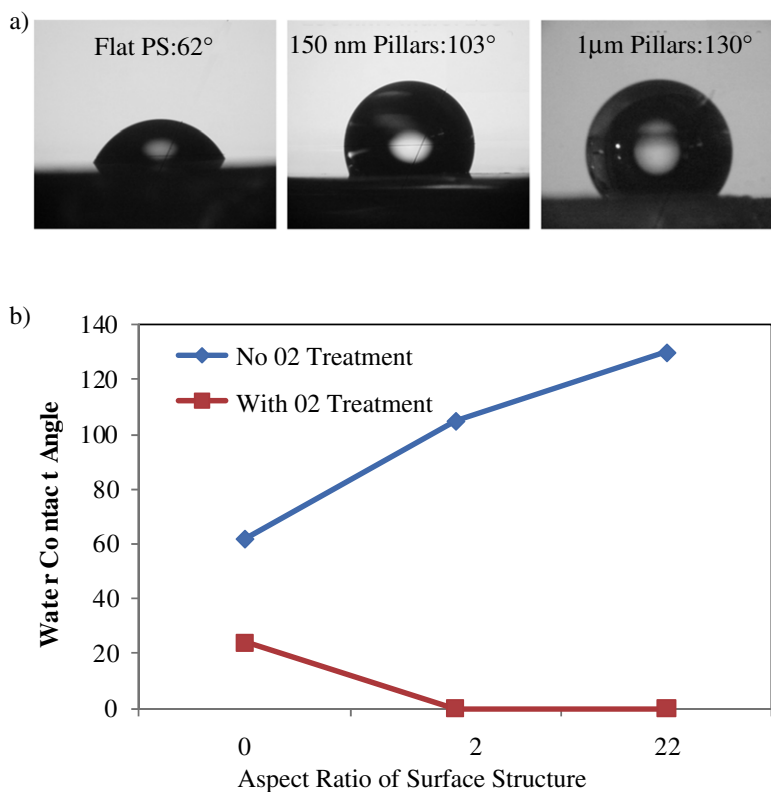


**Figure 3.** (a) Deionized water droplets placed on flat TCPS, 150 nm long, and 1 μm long pillars in TCPS, respectively. (b) The measured contact angles as a function of pillar aspect ratio with and without O<sub>2</sub> plasma treatment.

and DAPI using a staining kit (part # FAK100, Chemicon International) according to the manufacturer’s protocol. Substrates were washed with buffer to remove loosely bound

cells before imaging. Digital microphotographs of stained cellular actin and nuclei were obtained using an Olympus BX51 fluorescent microscope with 10× objective. Digital

microphotographs of the cells were also obtained using a light microscope with phase contrast. Cell areas were determined using the ImageJ graphic tool. For each substrate type, cell areas were measured on multiple substrate samples ( $n = 3\text{--}8$ ) or, in the case of the non-patterned  $\text{O}_2$ -treated surface, three discrete regions of a single substrate. At least 12 cells, and up to 50, were measured on each substrate or region. Only cells that were well separated from other cells so that their boundaries could be discerned were measured, which excluded a large number of cells on the pillared substrates that were clumped together. The mean cell area for each substrate or region was taken as the value for that region and the mean of those means for the multiple regions/substrates is reported for each substrate type. Error bars are the standard deviations in the means of different substrates/regions.

### 3. Results and discussions

figure 2(a) shows 150 nm tall pillars, 80 nm in diameter and 100 nm in pitch, which resulted from imprinting with partial filling of the 500 nm deep mold at 120 °C and a pressure of 40 bar for 5 min. Figure 2(b) shows 700 nm tall, 60 nm wide pillars, and figure 2(c) shows 1  $\mu\text{m}$  tall pillars of 40–50 nm diameter obtained by demold-induced elongation at 65–70 °C. Uniform nanopillars with aspect ratio of 20–25 (height much larger than the mold depth) were achieved reproducibly over large areas (figure 2(c)). Due to the very high aspect ratio, polystyrene pillars tend to bend and group together. The inset image in figure 2(c) shows the cross-sectional view of a tall pillar adjacent to a surface defect. Such long pillars cannot be made by conventional nanoimprint methods due to fundamental limits on aspect ratio set by polymer cohesion forces and mold-polymer adhesion during demolding [16]. Thus, creation of otherwise inaccessible surface topography is enabled by this novel methodology.

Macroscale surface properties such as surface energy and wettability depend on the nanoscale physical topography of the surface. Previous studies have addressed the wetting properties of solid surfaces as a function of surface roughness, creating both superhydrophobic and superhydrophilic surfaces by manipulation of topography [17–20]. Hydrophobic behavior on structured surfaces is observed for a liquid drop in a stable Cassie–Baxter state, characterized by stable air pockets separating the liquid from depressions in the substrate [21]. This state can be achieved by using high aspect ratio structures along with sharp pillar tips, which reduce the contact area between the pillar and liquid [17, 20].

The high aspect ratios (AR) achieved in this work impart extreme hydrophobicity to the surface, permitting a stable water drop. Figure 3(a) shows water droplets on flat TCPS (AR = 0), 150 nm pillars (AR  $\sim$  2), and 1  $\mu\text{m}$  pillars (AR  $\sim$  22). Figure 3(b) plots the water contact angle as a function of aspect ratio with and without  $\text{O}_2$  plasma treatment. The results confirm accepted theory, which states that for a constant shape structure, increasing aspect ratio enhances the hydrophobicity of the surface [20]. Higher aspect ratios simply ensure and enhance air trapping. On the other hand, the surface chemistry of the material clearly plays a significant

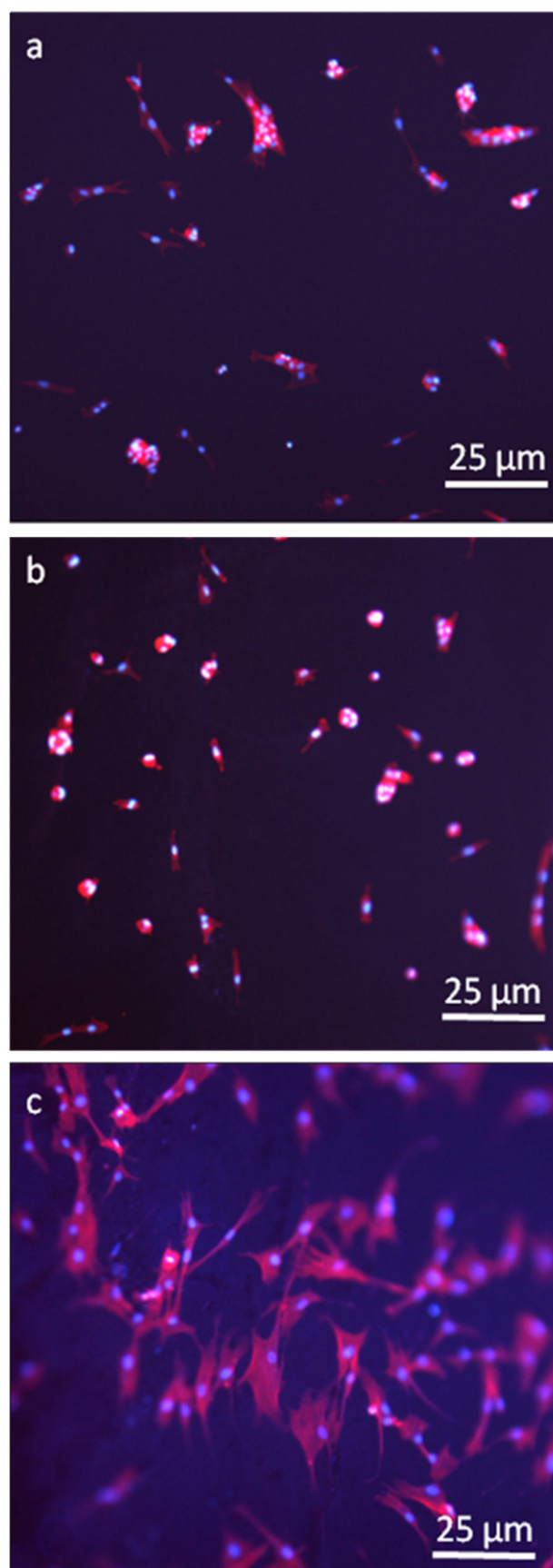


**Figure 4.** Fluorescent images of human dermal fibroblasts on nanopillars in TCPS: (a) pillar height of 150 nm; (b) pillar approaching 1  $\mu\text{m}$  in height; and (c) on flat TCPS.

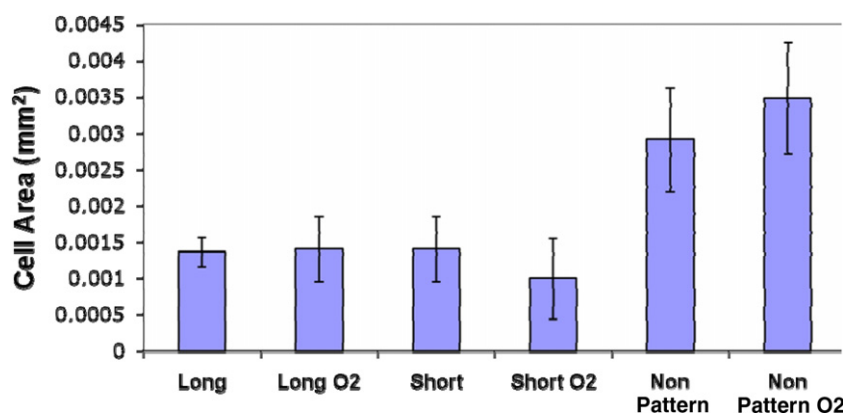


**Figure 5.** Averaged cell areas for 150 nm, 1000 nm tall nanopillars, non-patterned pillars, and with/without O<sub>2</sub> treatment.

role in the hydrophobicity of the pillar surface. Addition of hydroxyl groups at the TCPS surface was performed using a low power reactive ion etching (RIE) with an O<sub>2</sub> pressure of 200 mTorr and a power of 50 W for 25 s. Minimizing the power and process time reduces the etching of TCPS to less than 5 nm. Though leaving the topography almost intact, this treatment renders the surface hydrophilic, reducing the contact angle to zero for both 150 nm and 1  $\mu$ m tall pillars. This effect demonstrates the ability of the topography and surface chemistry to independently influence macroscale properties of the surface.

To investigate the concurrent effects of topography and surface energy on the cell–substratum interaction, TCPS nanopillars of widely varying aspect ratios and wettabilities were prepared. Human dermal fibroblasts were cultured on these substrates and their morphology was analyzed. Nuclei and cytoskeletal actin were observed by fluorescence microscopy after staining. The cells on nanopillars (figures 4(a) and (b)) displayed a fundamentally different morphology than cells on a flat control surface (figure 4(c)). They restricted themselves to a significantly smaller surface area, appearing spheroidal or having a highly polarized morphology of long protrusions with little spreading on the surface (figures 4(a) and (b)). In contrast, cells on flat control were polygonal and well spread (figure 4(c)). In addition, cells on the pillars seemed to aggregate, indicated by clusters of nuclei (figures 4(a) and (b)). Figure 5 shows the quantitative analysis of cell area for the surfaces tested, with and without the O<sub>2</sub> plasma treatment. The nanopillar topography resulted in a 40–50% reduction in cell area compared to a flat control. This result agrees with previous studies of cell growth on nanoscale pores and pillars [1, 11, 13, 14, 22]. Although the O<sub>2</sub> plasma treatment dramatically reduced the surface energy of nanopillar-imprinted polystyrene from highly hydrophobic to superhydrophilic, e.g. from a water contact angle of 130°–0° for tall pillars (figure 3), cell spreading on both tall and short nanopillars remained unaffected by this treatment (figure 5). This result addresses the possibility that poor cell spreading on the pillar surfaces is simply an effect of the surface energy, with the highly hydrophobic surface resisting cell spreading. The similar behavior (small cell area and aggregation of cells) observed on hydrophilic as well as hydrophobic pillar

surfaces suggests that the behavior results directly from the cell response to the nanoscale surface topography rather than to the surface hydrophobicity/hydrophilicity. An alternative interpretation is that cell spreading depends upon surface adsorption of extracellular proteins which itself requires an intermediate surface energy, neither too hydrophilic nor too hydrophobic. Our data do not rule out this possibility, but the similar spread morphology of cells on flat polystyrene with and without O<sub>2</sub> plasma treatment indicate that a wide range of surface energies will support spreading. Another possibility is that the imprinting process itself induces a chemical change in the polystyrene that results in reduced support for cell spreading. However, similar results have been observed on nanostructures of other materials, such as TiO<sub>2</sub> [11]. Thus we favor the interpretation that the high aspect ratio nanopillar topography itself resists spreading of adherent cells. It should be pointed out that important factors not considered in this study are the interaction forces between cell and substrate, which may explain the variations of observed cell behaviors on similar nanotopography but with different material stiffness [1, 11, 13, 14].

We previously reported that the aspect ratio of surface structures plays a critical role in cell–substratum interaction, irrespective of cell type or the lateral dimensions of surface structures [12]. We found that the alignment and elongation of dermal fibroblasts can respond to structures of a small aspect ratio ( $\sim 0.05$ ) and the effect saturates above a critical aspect ratio of  $\sim 0.5$  [12]. The results of the present study are consistent with this finding. The aspect ratios of the nanopillars reported here (AR  $\sim 22$  for 1  $\mu$ m pillars, AR  $\sim 2$  for 150  $\mu$ m pillar) are much larger than the critical value at which effects on cell spreading are maximized. Thus, although the aspect ratios of these surface features differ by an order of magnitude and their surface energies are appreciably different, we observe no difference in cell spreading between tall and short nanopillars.

The observed reduction in cell spreading on the nanopillar surfaces presumably results from failure of filopodia, by which cells explore their environment and direct spreading, to sense a conducive surface. Since filopodial protrusions can readily span the distances between nanopillars in this study [23], the inhibition of cell spreading likely indicates a low propensity for focal adhesions to form on the surface. Focal adhesions

are formed by the clustering of cell–surface integrins bound to the matrix into adhesion complexes. These adhesion complexes are much larger than the nm-scale tops of the pillars, on the micron size scale in fibroblasts [24]. Thus, in a model for the inhibited spreading of cells on the nanopillar surface, cytoskeletal rigidity confines extended filopodia to exploring the tops of the pillars, but there is insufficient continuous surface area at the tops of the pillars to support adequate integrin clustering for formation of effective adhesion complexes. The strength of cell adhesion being largely determined by the density and distribution of focal contacts formed at the surface [25–28], the observed aggregation of cells on the pillar surfaces might be a consequence of weak adhesion, with the cells that remain on the surface primarily those that cling cooperatively.

#### 4. Conclusions

We report a high-throughput method to enable the fabrication of high aspect ratio, high density polymer nanopillars ( $10^{10} \text{ cm}^{-2}$ ) in tissue culture polystyrene plates over large areas. Ultrahigh aspect ratio polymer pillars (longer than the mold depth) are obtained by utilizing demold-induced elongation. Both highly hydrophobic and superhydrophilic nanopillar surfaces were used as cell culture substrates, and cell morphology was assessed. Cells spread poorly on both the hydrophobic and hydrophilic nanopillars. The results can be rationalized in terms of the ability of the cells to form effective adhesion complexes on the restricted area at the tops of the pillars. This study demonstrates that nanostructuring is a feasible way to make surfaces that resist cell spreading and adhesion, which can be useful for cell culture, bio-MEMs, and implant devices where biological and abiological interfaces are involved.

#### Acknowledgment

This work is supported by the Texas Higher Education Coordinating Board through its Advanced Research Program under Contract No. 009741-0015-2006.

#### References

- [1] Sniadecki N, Desai R, Ruiz S and Chen C 2006 Nanotechnology for cell–substrate interactions *Ann. Biomed. Eng.* **34** 59–74
- [2] Davis S S 1997 Biomedical applications of nanotechnology—implications for drug targeting and gene therapy *Trends Biotechnol.* **15** 217–24
- [3] Wen X, Shi D and Zhang N 2005 Applications of nanotechnology in tissue engineering *Handbook of Nanostructured Biomaterials and their Applications in Nanobiotechnology* vol 2 (Stevenson Ranch, CA: American Scientific Publishers) pp 393–414
- [4] Wagner V, Dullaart A, Bock A K and Zweck A 2006 The emerging nanomedicine landscape *Nat. Biotechnol.* **24** 1211–7
- [5] Kwon J, Trivedi K, Krishnamurthy N V, Hu W, Lee J-B and Gimmi B 2009 SU-8-based immunoisolate microcontainer with nanoslots defined by nanoimprint lithography *J. Vac. Sci. Technol. B* **27** 2795–800
- [6] Andersson A, Backhed F, Euler Av, Richter-Dahlfors A, Sutherland D and Kasemo B 2003 Nanoscale features influence epithelial cell morphology and cytokine production *Biomaterials* **24** 3427–36
- [7] Clark P, Connolly P, Curtis A, Dow J and Wilkinson C 1991 Cell guidance by ultrafine topography *in vitro J. Cell Sci.* **99** 73–7
- [8] Teixeira A, Abrams G, Murphy C and Nealey P 2003 Cell behavior on lithographically defined nanostructured substrates *J. Vac. Sci. Technol. B* **21** 683–7
- [9] Loesberg W *et al* 2007 The threshold at which substrate nanogroove dimensions may influence fibroblast alignment and adhesion *Biomaterials* **28** 3944–51
- [10] Hu W, Yim E, Reano R, Leong K and Pang S W 2005 Effects of nanoimprinted patterns in tissue-culture polystyrene on cell behavior *J. Vac. Sci. Technol. B* **23** 2984–9
- [11] Park J, Bauer S, von der Mark K and Schmuki P 2007 Nanosize and vitality: TiO<sub>2</sub> nanotube diameter directs cell fate *Nano Lett.* **7** 1686–91
- [12] Crouch A S, Miller D, Luebke K J and Hu W 2009 Correlation of anisotropic cell behaviors with topographic aspect ratio *Biomaterials* **30** 1560–7
- [13] Curtis A, Gadegaard N, Dalby M, Riehle M, Wilkinson C and Aitchison G 2004 Cells react to nanoscale order and symmetry in their surroundings *IEEE Trans. Nanobiosci.* **3** 61–5
- [14] Dalby M, Riehle M, Sutherland D, Agheli H and Curtis A 2004 Changes in fibroblast morphology in response to nano-columns produced by colloidal lithography *Biomaterials* **25** 5415–22
- [15] Aryal M *et al* 2008 Imprinted large-scale high density polymer nanopillars for organic solar cells *J. Vac. Sci. Technol. B* **26** 2562–6
- [16] Tao L, Zhao X M, Gao J M and Hu W 2010 Lithographically defined uniform worm-shaped polymeric nanoparticles *Nanotechnology* **21** 095301
- [17] Bico J, Thiele U and Quere D 2002 Wetting of textured surfaces *Colloids Surf. A* **206** 41–6
- [18] Patankar N 2004 Mimicking the lotus effect: influence of double roughness structures and slender pillars *Langmuir* **20** 8209–13
- [19] Jung Y and Bhushan B 2006 Contact angle, adhesion and friction properties of micro- and nanopatterned polymers for superhydrophobicity *Nanotechnology* **17** 4970–80
- [20] Martinez E, Seunarine K, Morgan H, Gadegaard N, Wilkinson C and Riehle M 2005 Superhydrophobicity and superhydrophilicity of regular nanopatterns *Nano Lett.* **2** 2097–103
- [21] Cassie A and Baxter S 1944 Wettability of porous surfaces *Trans. Faraday Soc.* **40** 546–51
- [22] Krasteva N *et al* 2004 Influence of polymer membrane porosity on C3A hepatoblastoma cell adhesive interaction and function *Biomaterials* **25** 2467–76
- [23] Curtis A and Wilkinson C 1997 Topographical control of cells *Biomaterials* **18** 1573–83
- [24] Kato M and Mrksich M 2004 Using model substrates to study the dependence of focal adhesion formation on the affinity of integrin–ligand complexes *Biochemistry* **43** 2699–707
- [25] Berry C, Curtis A, Oreffo R, Agheli H and Sutherland D 2007 Human fibroblast and human bone marrow cell response to lithographically nanopatterned adhesive domains on protein rejecting substrates *IEEE Trans. Nanobiosci.* **6** 201–9
- [26] Allen T 2006 Preparation and maintenance of single-cell micro-island cultures of basal forebrain neurons *Nat. Protoc.* **1** 2543–50
- [27] Chen C, Ostuni E, Whitesides G and Ingber D 2000 Using self-assembled monolayers to pattern ECM proteins and cells on substrates *Meth. Mol. Biol.* **139** 209–19
- [28] Wilkinson C, Curtis A and Crossan J 1998 Nanofabrication in cellular engineering *J. Vac. Sci. Technol. B* **16** 3132–6